Conformational Analysis of a Flexible Oligosaccharide Using Residual Dipolar Couplings

Fang Tian, Hashim M. Al-Hashimi,‡ John L. Craighead,† and James H. Prestegard*

Contribution from the Complex Carbohydrate Research Center, The University of Georgia, 220 Riverbend Rd., Athens, Georgia 30602-4712

Received August 4, 2000. Revised Manuscript Received October 20, 2000

Abstract: We present a new approach to the analysis of the conformational and the motional properties of an oligosaccharide, methyl 3,6-di-*O*-(α-D-mannopyranosyl)-α-D-mannopyranoside. The approach relies on an order matrix analysis of residual dipolar couplings in the solution state. By combining a number of different types of couplings, $^1D_{CH}$, $^2D_{CH}$, and D_{HH}, an order matrix is solved for each ring of the trimannoside. The resulting order parameters indicate the internal motion at the α (1,3) linkage to be limited, while significant motion is suggested at the α (1,6) linkage. Two structures for the trimannoside were determined by aligning the order tensor principal axes obtained from two different orienting media, bicelles and phage. The very similar conformations at the α (1,3) linkage of these two structures confirm that the internal motion at the α (1,3) linkage is small and the conformation is a good representation of a single preferred structure. The different conformations at the α (1,6) linkage suggest that the motional amplitudes are large and the conformations must be viewed as virtual conformers. Compared with traditional NMR methods, data acquisition is easy and data analysis is straightforward.

Introduction

Carbohydrates play a variety of roles in all forms of life. They serve as energy stores, structural elements of the cell walls of bacteria and plants, and participants in a host of cell recognition phenomena.[1−3] Despite their importance, structural characterizations of these molecules in aqueous solution have been challenging; traditional NMR methods based on NOEs and scalar couplings typically yield a limited number of structural constraints,[4−9] and data interpretation is often complex, especially in the presence of internal motion. The inherent conformational flexibility of carbohydrates, which is believed to be important for their biological function, has been investigated extensively using ^{13}C spin relaxation measurements.[10,11] Spin relaxation measurement can give estimates of time scales and amplitudes of motion, but primarily for motion on time scales shorter than ∼1 ns. Recently, examples of using residual dipolar couplings to study carbohydrates have appeared.[12−17] The focus so far has been on structural application, but this alternate approach offers some interesting possibilities for characterizing amplitudes of motion as well. Here we apply the new approach in the analysis of both the conformational and motional properties of an oligosaccharide.

Dipolar couplings arise from through space spin−spin interactions and depend on both internuclear distance (r) and an angle between the magnetic field and the internuclear vector (θ) as described by the equation

$$D_{ij} = \xi_{ij}\left\langle\frac{(3\cos^2\theta - 1)}{2}\right\rangle(1/r^3)$$

where ξ_{ij} is a constant that depends on the properties of nuclei i and j. The dipolar couplings contain both short-range (distance-dependent) and long-range (angular-dependent) structural information. In traditional NMR experiments, the internuclear vector samples orientations isotropically as a result of free tumbling in aqueous solution, thus the $(3\cos^2\theta - 1)$ term is averaged to zero and the possibility of a direct measurement of angular information disappears. The distance dependence can still be retrieved, but only indirectly through relaxation phenomena such as the nuclear Overhauser effect (NOE). For many molecules indirect measurement has been adequate. In fact, measurement of interproton NOEs has become the foundation of biomolecular

* To whom correspondence should be addressed.
‡ Current address: Cellular Biochemistry and Biophysics Program, Memorial Sloan-Kettering Cancer Center, New York, NY 10021.
† Current address: Scripps Research Institute, La Jolla, CA 92037.

(1) Dumitriu, S. E. *Polysaccharides*: *Structural Diversity and Funtional Versatility*; Marcel Dekker: New York, 1998.
(2) Lasky, L. A. *Science* **1992**, *258*, 964−969.
(3) Varki, A. *Glycobiology* **1993**, *3*, 97−130.
(4) Tvaroska, I.; Hricovini, M.; Petrakova, E. *Carbohydr. Res.* **1989**, *189*, 359−362.
(5) Jiménez-Barbero, J.; Asensio, J. L.; Cañada, F. J.; Poveda, A. *Curr. Opin. Struct. Biol.* **1999**, *9*, 549−555.
(6) Poveda, A.; Jiménez-Barbero, J. *Chem. Soc. Rev.* **1998**, *27*, 133−143.
(7) Bose, B.; Zhao, S.; Stenutz, R.; Cloran, F.; Bondo, P. B.; Bondo, G.; Hertz, B.; Carmichael, L.; Serianni, A. S. *J. Am. Chem. Soc.* **1998**, *120*, 11158−11173.
(8) Xu, Q. W.; Bush, C. A. *Biochemistry* **1996**, *35*, 14521−14529.
(9) van Halbeek, H. *Curr. Opin. Struct. Biol.* **1994**, *4*, 697−709.
(10) Rundlöf, T.; Venable, R. M.; Pastor, R. W.; Kowalewski, J.; Widmalm, G. *J. Am. Chem. Soc.* **1999**, *121*, 11847−11854.
(11) Mäler, L.; Widmalm, G.; Kowalewski, J. *J. Phys. Chem.* **1996**, *100*, 17103−17110.
(12) Martin-Pastor, M.; Bush, C. A. *Biochemistry* **2000**, *39*, 4674−4683.
(13) Martin-Pastor, M.; Bush, C. A. *Carbohydr. Res.* **2000**, *323*, 147−155.
(14) Rundlëf, T.; Landersjö, C.; Lycknert, K.; Maliniak, A.; Widmalm, G. *Magn. Reson. Chem.* **1998**, *36*, 773−776.
(15) Kiddle, G. R.; Homans, S. W. *FEBS Lett.* **1998**, *436*, 128−130.
(16) Bolon, P. J.; Al-Hashimi, H. M.; Prestegard, J. H. *J. Mol. Biol.* **1999**, *293*, 107−115.
(17) Shimizu, H.; Donohue-Rolfe, A.; Homans, S. W. *J. Am. Chem. Soc.* **1999**, *121*, 5815−5816.

10.1021/ja002900l CCC: $20.00
Published on Web 12/19/2000

structure determination by traditional NMR.[18] For moderate size molecules such as oligosaccharides, however, NOE transfer is not efficient and can even go to zero regardless of the internuclear distances because of the correlation time dependence of cross-relaxation. If the molecules are not rigid, as in the case of most oligosaccharides, the interpretation of NOEs can also be problematic.

Recent advances in high-resolution NMR spectroscopy allow direct measurements of dipolar interactions by dissolving molecules in oriented media such as liquid crystals composed of bicelles or phage.[19−22] Though molecular tumbling remains fast in these media, which preserves high-resolution spectra, the sampling of orientations is no longer isotropic. As a result, the dipolar couplings do not average to zero and splittings are observed between the dipolar coupled spin pairs. When internuclear distances are known, as in directly bonded $^{13}C-^{1}H$ or $^{15}N-^{1}H$ spin pairs, the dipolar couplings can provide new angular dependent information for investigating biomolecule structure and dynamics.[20,23−25]

In this study we use an order matrix analysis of residual dipolar couplings to study both the structure and flexibility of our target oligosaccharide. This approach requires knowledge of molecular geometry of a fragment that can be assumed rigid (or exhibits only small local librations), as well as measurements of five or more independent residual dipolar couplings from the fragment. This allows determination of Saupe order matrix elements (S_{ij}) from a set of linear equations relating dipolar couplings to the known geometry factors and the unknown order tensor elements.[26]

$$D_{\text{resid}} \propto \sum_{i,j} S_{ij} \cos\theta_i \cos\theta_j$$

Here, $\theta_{i,j}$ are the angles between the internuclear vectors and the *i*th (or *j*th) axis of an arbitrary molecular frame. Diagonalization of the Saupe matrix yields a principal order parameter (S_{zz}) and an asymmetry parameter ($\eta = |(S_{yy} - S_{xx})/S_{zz}|$), as well as a rotation matrix **R**, which relates the arbitrary starting molecular fragment frame to the principal order tensor frame.

Determinations of the Saupe order matrices for individual rigid fragments of a molecule allow both structural characterizations and assessments of internal motions between fragments. The former arises because molecular fragments must share a common order tensor frame if a single rigid model exists, while the latter arises because the determined order parameters will reflect overall averaging of the molecule as well as averaging due to internal motions. A parameter ϑ, called the Generalized Degree of Order (GDO), has been introduced as a single quantity that describes molecular order in terms of Saupe order matrix elements[25,27]

$$\vartheta = \sqrt{\frac{2}{3}\sum_{ij} S_{ij}^{\,2}}$$

Unlike S_{zz} which only reflects order about the *Z* axis, the GDO allows a characterization of the degree of internal motion independent of the choice of an order frame and independent of the level of anisotropy of motion. While comparison of order parameters for each principal axis can be done, a single number which reflects overall motion is convenient. For rigidly connected molecular fragments, GDO values (as well as the individual order parameters) are identical for all fragments. However, in the presence of internal motions between fragments, the GDO values will be attenuated by an amount that depends on the amplitude of motion, much like a spin relaxation order parameter. However, because residual dipolar couplings are sensitive to all motions that occur on time scales faster than approximately 1 ms, the GDO is sensitive to the presence of motions that may go undetected in spin relaxation studies.

One small remaining problem originates from an inability to uniquely determine axis directions when seeking alignment of fragment frames. Because of the inherent $\cos^2\theta$ dependence of dipolar couplings, dipolar couplings are insensitive to inversion of any pair of axes. Hence four alignments are allowed. This ambiguity can be eliminated by measurement of order tensor in a second alignment medium—a practice we exercise here using bicelle and phage based alignment media.[28]

The above formalism is ideal for studying the conformations of flexible carbohydrate molecules. Here, individual pyranose rings can be considered to be fragments, whose internal geometry is approximately known and which can to a good approximation be considered rigid. The above formalism can be applied to explore the structure and internal motions of these notoriously flexible molecules, providing measurement of five or more residual dipolar couplings per pyranose ring is possible. To accomplish this we examine a number of different types of couplings, $^{1}D_{CH}$, $^{2}D_{CH}$, and D_{HH}, in what follows.

Methyl 3,6-di-*O*-(α-D-mannopyranosyl)-α-D-mannopyranoside (trimannoside, Figure 1) will be used to illustrate the utility of residual dipolar coupling information in this work. This trimannoside forms a common core in N-linked oligosaccharides. Three mannoses are connected together through two of the most commonly found glycosidic linkages, α (1,3) and α (1,6). This molecule has been studied previously by ourselves and others using conventional NMR methods.[29,30] The most recent proposed structural model describes its conformation as an average of four major forms arising from a pair of two-state transitions, with (ϕ, ψ) = (60°, −180°) and (80°, −100°) at the α(1,3) and (ϕ, ψ, ω) = (64°, 180°, 60°) and (64°, 180°, 180°) at the α(1,6) linkages. The transition at the α(1,3) is fast and changes the molecular shape slightly, while the transition at the α(1,6) is much slower and alters the molecular shape dramatically.[30] The results obtained with our new approach prove to be in good agreement with those studies but also provide new insights into the distribution of conformers sampled by trimannoside in aqueous solution.

Results

Measurement of Residual Dipolar Couplings in Bicelle and Phage Solutions. Most of our previous studies of oligosac-

(18) Wüthrich, K. *NMR of Proteins and Nucleic Acids*; Wiley: New York, 1986.
(19) Prestegard, J. H. *Nat. Struct. Biol.* **1998**, *5*, 517−522.
(20) Tjandra, N.; Bax, A. *Science* **1997**, *278*, 1111−1113.
(21) Hansen, M. R.; Muller, L.; Pardi, A. *Nat. Struct. Biol.* **1998**, *5*, 1065−1074.
(22) Clore, G. M.; Starich, M. R.; Gronenborn, A. M. *J. Am. Chem. Soc.* **1998**, *120*, 10571−10572.
(23) Clore, G. M.; Gronenborn, A. M. *Proc. Natl. Acad. Sci. U.S.A.* **1998**, *95*, 5891−5898.
(24) Tolman, J. R.; Flanagan, J. M.; Kenedy, M. A.; Prestegard, J. H. *Proc. Natl. Acad. Sci. U.S.A.* **1995**, *92*, 9297−9283.
(25) Prestegard, J. H.; Tolman, J. R.; Al-Hashimi, H. M.; Andrec, M. In *Biological Magnetic Resonance*; Krishna, N. R., Berliner, L. J., Eds.; Plenum: New York, 1999; Vol. 17, pp 311−355.
(26) Saupe, A. *Angew. Chem., Int. Ed. Engl.* **1968**, *7*, 97.
(27) Prestegard, J. H.; Al-Hashimi, H. M.; Tolman, J. R. *Q. Rev. Biophys.* **2000**, in press.
(28) Al-Hashimi, H. M.; Valafar, H.; Terrell, M.; Zartler, E. R.; Eidsness, M. K.; Prestegard, J. H. *J. Magn. Reson.* **2000**, *143*, 402−406.
(29) Brisson, J.-R.; Carver, J. P. *Biochemistry* **1983**, *22*, 1362−1368.
(30) Sayers, E.; Prestegard, J. H. *Biophys. J.* **2000**, in press,

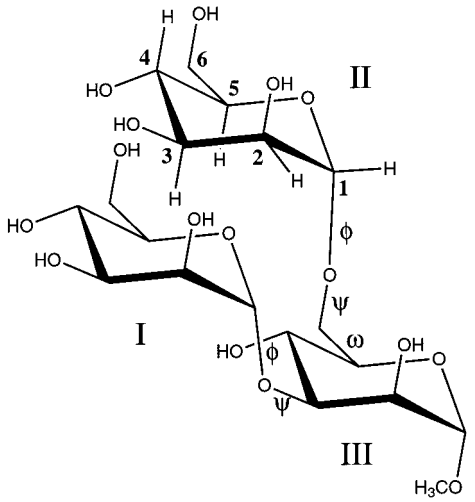

Figure 1. Structure of trimannoside, methyl 3,6-di-*O*-(α-D-mannopyranosyl)-α-D-mannopyranoside. Rings are labeled with Roman numerals. The IUPAC convention is used for defining the torsion angles: $\phi = O5(i)-C1(i)-On(i-1)-Cn(i-1)$, $\psi = C1(i)-On(i-1)-Cn(i-1)-C(n-1)(i-1)$, $\Omega = O6(i)-C6(i)-C5(i)-C4(i)$, Where ($i$) indicates a given residue and (n) a ring position.

charides have employed ^{13}C enrichment.[16,31] With recent improvements in sensitivity of NMR experiments, this is not required. The ^{13}C constant time coupling enhanced HSQC (CT-CE-HSQC) spectra of the target trimannoside at natural abundance are shown in Figure 2 (assignments were obtained from our previous NOE and scalar coupling based studies[30]). The resonances are well resolved except for the H4 protons of rings I and II. In this experiment, the one-bond $^{13}C-^{1}H$ couplings evolved for a full t_1 increment while the chemical shifts evolved for only half of the increment; hence the $^{13}C-^{1}H$ splittings appear doubled. These spectra were acquired at 800 MHz to minimize second-order effects on splittings of ring protons. The measured one-bond $^{13}C-^{1}H$ residual dipolar couplings are listed in Table 1. Both positive and negative values were observed, ranging from +16.5 to −17.4 Hz for the bicelle sample and from +5.5 to −4.2 Hz for the phage sample. The nearly parallel vectors of the C3−H3, C4−H4, and C5−H5 bonds for mannose are reflected in the similar sizes of the dipolar couplings. While the data are of high quality, the near degeneracy in vector direction makes it difficult to get five independent dipolar couplings measurements from this experiment alone.

The vectors connecting proximate protons of the sugar rings are not typically parallel to the one-bond $^{13}C-^{1}H$ vectors. The $^{1}H-^{1}H$ couplings can be accurately measured by a simple constant time COSY (CT-COSY) experiment.[32] Since this experiment has very good sensitivity, several spectra with various constant time delays were recorded and data were fit to the equation

$$\frac{I_{\text{cross}}}{I_{\text{auto}}} = A \tan(\pi(J + D)t)$$

relating the intensity ratios of cross-peaks and auto-peaks to a function of the constant time delays (t). The extracted values for $^{1}H-^{1}H$ couplings (D) are also listed in Table 1. Only couplings for H1−H2 and H2−H3 of each ring are reported, since these protons are best resolved in 2D homonuclear CT-COSY spectra. Resolution of additional peaks can be achieved through the use of a ^{13}C-edited CT-COSY experiment, but the sensitivity of this experiment on the natural abundant trimannoside is low. The signs of couplings cannot be determined from CT-COSY experiments unless large scalar couplings of known sign exist for the pair of protons. For most cases discussed here, this was not the case, and two possible values of each $^{1}H-^{1}H$ dipolar coupling resulted. Such ambiguities did not prove to be a problem during order matrix calculations, as in all cases only a single combination of the possible values yielded solutions. In Table 1 there are also two 0 Hz $^{1}H-^{1}H$ couplings listed for each ring because no cross-peaks were observed between these spin pairs. The distances between these spin pairs are less that 4.2 Å, a distance that should have produced observable cross-peaks in the aligned media if the angular factor was not near zero.

As trimannoside was aligned to a lesser extent in phage solution, it proved useful to seek additional constraints for this medium. Two-bond $^{13}C-^{1}H$ dipolar couplings were measured to provide the additional experimental constraints. These couplings were measured using an E. COSY type experiment,[33,34] thus the sign of these couplings could be determined based on the positive sign of one-bond $^{13}C-^{1}H$ couplings. The measured two-bond $^{13}C-^{1}H$ dipolar couplings are much smaller, ranging from +0.6 to −0.7 Hz with a precision of 0.4 to 0.8 Hz; they are nevertheless useful and are therefore listed in Table 1 as well.

Order Matrix Analysis of the Residual Dipolar Couplings. Ring geometry factors based on an arbitrary coordinate frame were input to the ORDERTEN_SVD program along with the measured residual dipolar couplings for one ring at a time.[35] The orientations of the resulting order tensor principal axis systems in bicelle media relative to the initial molecular frame are shown in Figure 3a for each ring using a Sauson−Flaumsteed projection. Each spot in these plots represents an allowed solution. Distribution of spots is a result of uncertainties in measurements of the dipolar couplings as well as uncertainty in local ring geometry. The top and the bottom tips of the map represent $+Z$ and $-Z$ in the initial coordinate frame while $+X$ is in the center pointing out of the page. The positions of the clusters of points can be related to Euler angles that transform the order axis to the arbitrary ring axis. The histograms showing the order parameter (S_{zz}) along with the asymmetry parameter (η) are presented in Figure 3a as well. For all three rings, the directions of highest order are well defined but there is a variation in position from ring to ring. The order parameters (S_{zz}, η) are (0.000 43, 0.40) for ring I, (0.000 33, 0.35) for ring II, and (0.000 48, 0.68) for ring III.

The order tensor of trimannoside in phage media was also determined from the measured residual dipolar couplings and the same initial molecular frame of mannose (Figure 3b). The order parameters (S_{zz}, η) here are (0.000 14, 0.50) for ring I, (0.000 12, 0.80) for ring II, and (0.000 17, 0.58) for ring III. The principal order frames of trimannoside in bicelle and phage media point in different directions based on an examination of the respective Sauson−Flaumsteed diagrams. In this case, the two independent order frames can be used to resolve orientational ambiguities. Moreover, they provide additional information on inter-ring motions.

(31) Aubin, Y.; Prestegard, J. H. *Biochemistry* **1993**, *32*, 3422−3428.
(32) Tian, F.; Bolon, P.; Prestegard, J. *J. Am. Chem. Soc.* **1999**, *121*, 7712−7713.
(33) Willker, W.; Leibfritz, D. *J. Magn. Reson.* **1992**, *99*, 421−425.
(34) Sørensen, M.; Meissner, A.; Sørensen, O. *J. Biomol. NMR* **1997**, *10*, 181−186.
(35) Losonczi, J. A.; Andrec, M.; Fischer, M. W. F.; Prestegard, J. H. *J. Magn. Reson.* **1999**, *138*, 334−342.

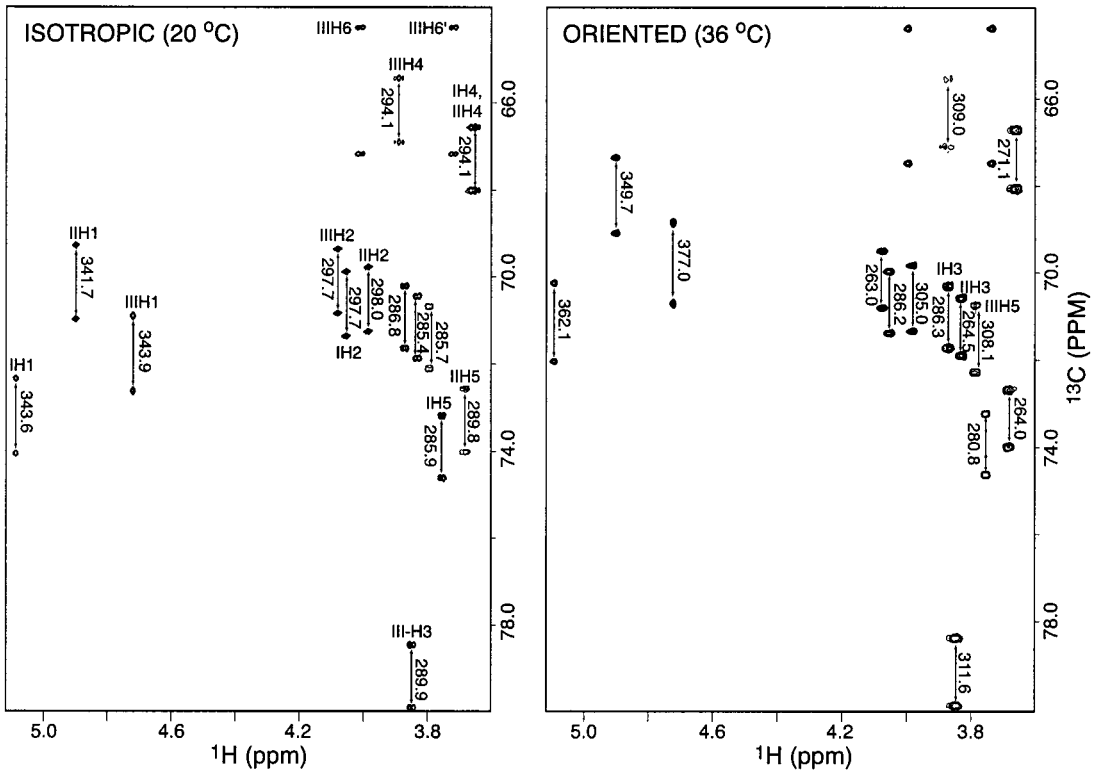

Figure 2. Constant time, coupling enhanced HSQC (CT-CE-HSQC) spectra of trimannoside in dilute bicelle media at 20 and 36 °C. The differences between the measured couplings in these two spectra result from the contributions of the residual dipolar couplings.

Discussion

The resulting principal order frames and order parameters can now be used to reconstruct an average geometry for trimannoside as well as investigate the inter-ring motions.[25,36] As described above, if two mannose rings were rigidly connected and linked with the proper geometry, the order parameters should be equivalent and the alignment tensors should superimpose. Any internal motion will result in additional averaging of the dipolar couplings and will reduce principal order parameters. While structure determinations based on superposition of the order tensor frames of fragments are rigorously valid for rigid molecules, it has also been shown by Tolman et al. that in the limit of moderate internal motions, aligning order tensor frames also leads to determination of a reasonable average geometry.[27] In the presence of more extensive motion (>30°, amplitude motions), assembling fragments based on aligning order tensor frames can lead to deviations from ideal geometries. For example, if complete rotational freedom exists about a particular bond, the axis of the highest order of the resulting order tensor would always be along this bond regardless of the orientation of the overall order tensor frame. Thus, it is important to screen for the presence of internal motion, and the GDO proves to be a useful tool in this respect. The GDOs for ring I, ring II, and ring III are 0.00044, 0.00034, and 0.00052, respectively, in bicelle media and 0.00015, 0.00013, and 0.00018, respectively, in phage media. The small difference in GDO values for rings I and III suggests the internal motion at this linkage is likely to be limited, while the nearly 40% and 30% differences in GDO values for rings II and III in bicellle and phage media indicate there is a more significant motion at this linkage. This is consistent with previous studies of this molecule by conventional NMR methods and molecular modeling.[29,30]

I−III Linkage. Since the internal motion at the α(1,3) linkage appears to be small, it should have little effect on the determined orientations of the principal axis of the order tensors. It is then appropriate to align order tensor frames to assemble a structure. Rings I and III can be oriented such that the principal axes of the alignment tensors in bicelle media (Figure 3a) coincide in four possible ways. The number of viable possibilities is reduced because ring I must be connected with ring III through translations such that the O1 of ring I superimposes with O3 of ring III and an appropriate bond angle is maintained. Two out of the four possible orientations prove to be disallowed because of bond geometry violations.

The remaining possible solutions can be distinguished by using the dipolar data collected from phage aligned media.[28] When one of the two conformers from the bicelle data is used as a starting point, coincidence of order frames from the phage data is not maintained (data not shown). The only allowed orientation of the ring I relative to ring III determined from bicelle data is shown in Figure 4a. The IC1−O−IIIC3 angle is 118°, in agreement with normal bond geometry. The torsion angles (ϕ,ψ) at the glycosidic bond are (67°, −103°), which are very similar to those of one of the major conformers (80°, −100°) proposed in our previous studies.[30] The X-ray structure of trimannoside bound to Concanavalin A is (70°, −115°) for (ϕ,ψ) at the α(1,3) linkage (code: 1CVN).[37]

The ring I−ring III junction was also assembled by aligning the order tensor principal axis determined from phage media, shown in Figure 4b. The fact that conformers derived from bicelle and phage data are very similar suggests they are viable structures and also indicates that the internal motion at the α-(1,3) linkage is small. A further piece of evidence to support the above structure comes from a transglycosidic ^{1}H−^{1}H coupling. The inter-ring proton−proton residual dipolar coupling of IH1−IIIH3 was calculated to be −2.6 Hz by using the

(36) Tolman, J. R.; Al-Hashimi, H. M.; Kay, L. E.; Prestegard, J. H. *J. Am. Chem. Soc*. Submitted for publication.

(37) Naismith, J. H.; Field, R. A. *J. Biol. Chem.* **1995**, *271*, 972−976.

Table 1. Residual Dipolar Couplings (RDC) for Trimannoside in Aligned Media

	RDC from 10% bicelle (Hz)	RDC from phage solution (Hz)
Ring I		
IC1−IH1	9.3 ± 1.0	2.3 ± 1.0
IC2−IH2	−5.8 ± 1.0	0.3 ± 1.0
IC3−IH3	−0.2 ± 3.0	−0.4 ± 3.0
IC5−IH5	−3.0 ± 3.0	−3.9 ± 3.0
IH1−IH2	1.9[a] or −5.3 ± 0.4	0.5[a] or −3.9 ± 0.2
IH2−IH3	3.65[a] or −10.59 ± 0.3	1.37[a] or −8.31 ± 0.1
IH1−IH3	0.0 ± 1.0	0.0 ± 1.0
IH1−IH4	0.0 ± 1.0	0.0 ± 1.0
IC1−IH2		0.1 ± 0.6
IC2−IH1		0.0 ± 0.4
IC3−IH2		−0.1 ± 0.6
Ring II		
IIC1−IIH1	4.0 ± 1.0	1.0 ± 1.0
IIC2−IIH2	3.5 ± 1.0	3.0 ± 1.0
IIIC3−IIH3	−10.9 ± 3.0	−2.6 ± 3.0
IIIC5−IIH5	−12.9 ± 3.0	−3.3 ± 3.0
IIH1−IIH2	2.86[a] or −6.44 ± 0.1	0.4[a] or −4.0 ± 0.2
IIH2−IIH3	1.3[a] or −8.3 ± 0.3	0.86[a] or −7.80 ± 0.1
IIH1−IIH4	0.0 ± 1.0	0.0 ± 1.0
IIH1−IIH5	0.0 ± 1.0	0.0 ± 1.0
IIC1−IIH2		0.6 ± 0.6
IIC2−IIH1		0.2 ± 0.5
Ring III		
IIIC1−IIIH1	16.5 ± 1.0	5.5 ± 1.0
IIIC2−IIIH2	−17.4 ± 1.0	−4.1 ± 1.0
IIIC3−IIIH3	10.9 ± 3.0	1.9 ± 3.0
IIIC4−IIIH4	7.4 ± 3.0	2.2 ± 3.0
IIIC5−IIIH5	11.2 ± 3.0	2.6 ± 3.0
IIIH1−IIIH2	−2.6[a] or −0.8 ± 0.5	−1.7 ± 0.4
IIIH2−IIIH3	4.1[a] or −10.5 ± 0.3	1.7[a] or −8.2 ± 0.2
IIIH1−IIIH3	0.0 ± 1.0	0.0 ± 1.0
IIIH1−IIIH4	0.0 ± 1.0	0.0 ± 1.0
IIIC1−IIIH2		−0.7 ± 0.6
IIIC2−IIIH1		0.0 ± 0.5
IIIC3−IIIH2		0.6 ± 0.6
IIIC3−IIIH4		−0.1 ± 0.6
IH1−IIIH3	±2.8 ± 0.5	

[a] Values yield solutions in order matrix calculations.

common alignment tensor and the proposed structure. This agrees well with the measured value of ±2.8 Hz.

In the above analysis, the center of each cluster of spots was used for the principal axes orientations of the order tensors. While the direction of highest order (S_{zz}) was well defined, there was frequently significant dispersion of directions for S_{xx} and S_{yy} (Figure 3a,b). For instance, uncertainties associated with directions for S_{xx} and S_{yy} of ring I in bicelle medium were ±25°. However, if we require the normal bond geometry at the glycosidic bond (C−O−C) to be 118° ± 5°, uncertainties in directions for S_{xx} and S_{yy} are reduced to ±10°.

Differences in GDOs provide a general indicator of internal motion about the I−III linkage (0.000 44 for ring I and 0.000 52 for ring III). However, an examination of S_{zz} and η separately can give insight into the nature of the motion. While ring I and ring III have similar S_{zz} values (slightly smaller for ring I), the asymmetry parameter is different with $\eta = 0.40$ for ring I and $\eta = 0.68$ for ring III. Motions with the rotor axis nearly parallel to the S_{zz} axis will affect η but leave S_{zz} less perturbed. The principal axis systems of order tensors determined from the bicelle data are superimposed on rings I and III in Figure 4a. The S_{zz} axis approximately points along the α(1,3) linkage; thus, the limited motion is approximately about the linkage, probably a combination of ϕ,ψ rotations. We can estimate the amplitude of this motion if we assume the ring III order parameters to represent overall molecular order. This may be a good assumption since the motion at the α(1,3) is fast and only changes the molecular shape slightly.[30] If the motion was a two-site jump about a single axis, a ±25° jump in the S_{zz} and S_{xx} plane and to either side of an axis that is 30° away from S_{zz} reduced η from 0.68 to 0.38 and S_{zz} from 0.000 48 to 0.000 42.

II−III Linkage. The GDO of ring II indicates that there is a more significant internal motion at the α(1,6) linkage. Depending on the nature of the motion, the order parameters as well as the orientations of the principal axis of the alignment tensor can be affected. If we insist on superimposing the principal axis of the order tensors of rings II and III, the assembled structure will be only a motionally averaged, "virtual" representation. This is shown in Figure 5a for bicelle data. In assembling this linkage, a ϕ angle of 64° was used (consistent with previous studies). Allowing the dipolar data to dictate other torsion angles at the glycosidic bond, one finds (164°, 100°) for (Ω, ψ). This is a significant departure from the major conformers proposed in previous studies (180°, 60°) and (180°, 180°). However, it is significant that our experimentally determined value of ψ lies between the ψ values for the major conformers.

The average structure of trimannoside for the α(1,6) linkage was also assembled by aligning the order tensor principal axis determined from phage media, and the results are shown in Figure 5b. Ring III has been superimposed with that in Figure 5a. The ring II orientations clearly appear different when viewed in the two media. Virtual conformers can look different when aligned in different media as internal motion will average dipolar couplings differently, particularly when motional amplitudes are large. A detailed analysis of the conformation behavior at this linkage requires identification of both proper sets of conformers and population distributions. Other than to say that conformers differ significantly and are both well populated, we leave this analysis for future studies.

In conclusion, we have presented a new method for the study of flexible carbohydrates. The GDO proves to be a good general indicator of the presence of internal motion. Variations of the alignment tensors determined in different media can also provide evidence of large-amplitude internal motions. In cases where only limited motion is present, however, a good representation of an average structure can be obtained by aligning order tensors and amplitudes of motion can be estimated. Compared with traditional NMR methods, the analysis is straightforward and both structural and motional information can be obtained.

Experimental Section

Sample Preparation. Trimannoside was purchased from Glycorex AB (Lund, Sweden) and used without further purification. This was dissolved in both bicelle and bacteriophage media for this study. The bicelle sample was 20 mM trimannoside in D_2O with 10% (w/v) DMPC/DHPC, 3:1 molar ratio, which gave an 18 Hz splitting of the ^2H NMR signal of D_2O at 36 °C. The preparation of bicelles is described elsewhere.[38] The phage sample contained 25 mM trimannoside in H_2O with enough phage to give an 13 Hz splitting of the ^2H NMR signal of D_2O at 36 °C. Pf1 phage was purified following the procedure of Hansen et al.[39]

NMR Spectroscopy. All data were acquired on Varian Inova spectrometers operating at 500 or 800 MHz for protons. The one-bond $^{13}C-^1H$ couplings were measured by using the constant time coupling enhanced HSQC (CT-CE-HSQC) sequence shown in Figure 6. This sequence is very similar to a normal CT-HSQC experiment.[40] The modification employs a pulse scheme that lets chemical shifts evolve

(38) Losonczi, J.; Prestegard, J. H. *J. Biomol. NMR* **1998**, *12*, 447−451.
(39) Hansen, M. R.; Mueller, L.; Pardi, A. *Nat. Struct. Biol.* **1998**, *5*, 1065−1074.
(40) Santoro, J.; King, G. C. *J. Magn. Reson.* **1992**, *97*, 202−207.

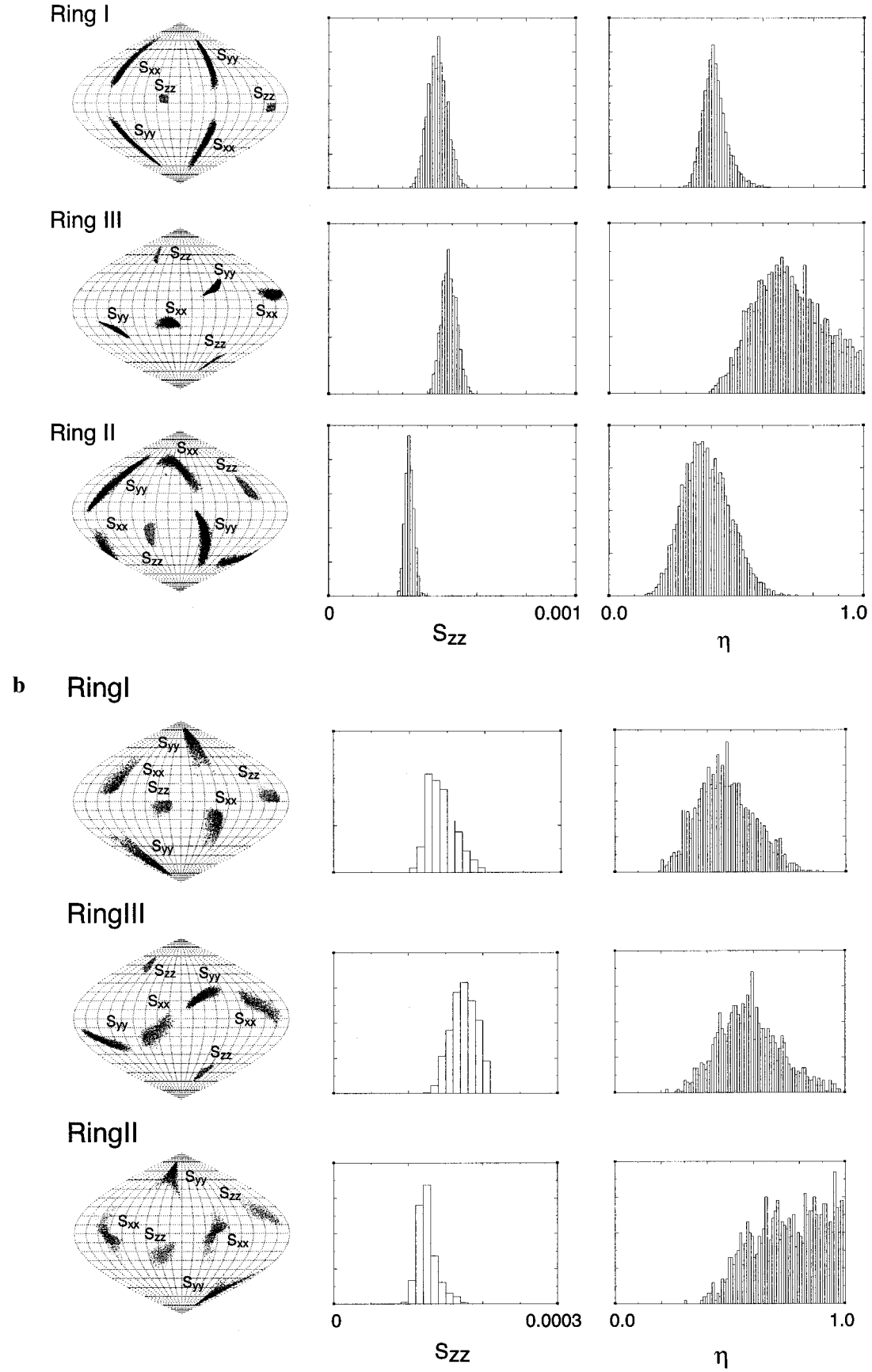

Figure 3. The alignment tensors for each individual ring of trimannoside in (a) bicelle and (b) phage determined separately from order matrix calculations. Sauson−Flamsteed projects show the orientations of the alignment tensor principal axis system in the initial molecular frame. The same arbitrary molecular frame is used for calculations on each ring. The histograms show the resulting order parameters S_{zz} and η.

one t_1 while the $^{13}C-^{1}H$ couplings evolve $2t_1$ during the indirect constant time period. Therefore, the $^{13}C-^{1}H$ splittings are doubled without an increase in line width, which in turn improves the precision of measurements in t_1 sampling limited applications by a factor of

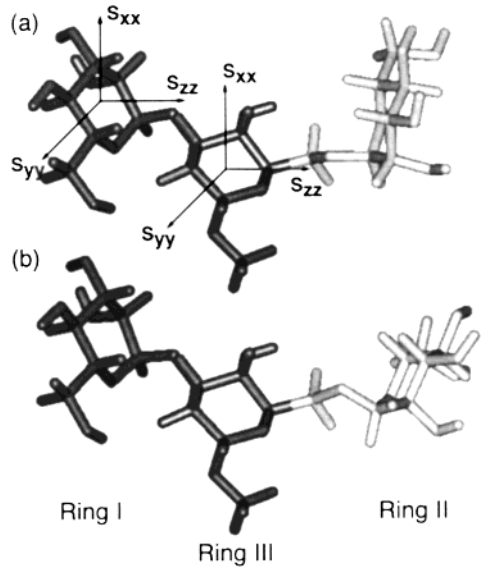

Figure 4. (a) The average structure of trimannoside ring I and ring III assembled by aligning the order tensor principal axis determined from bicelle media. Superimposed on ring I and ring III are coordinate frames representing the order tensor principal axis determined separately for each ring. (b) The average structure of trimannoside ring I and ring III assembled by aligning the order tensor principal axis determined from phage media. The structure is oriented to show the similarity of conformations about the α (1,3) linkage.

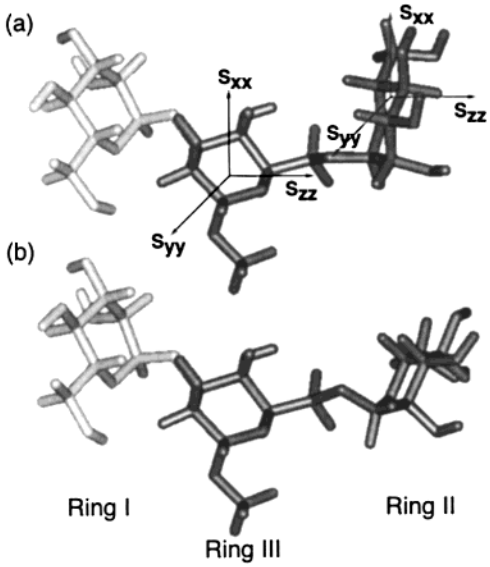

Figure 5. (a) The average structure of trimannoside ring II and ring III assembled by aligning the order tensor principal axis determined from bicelle media. Superimposed on ring II and ring III are coordinate frames representing the order tensor principal axes determined separately for each ring. (b) The average structure of trimannoside ring II and ring III assembled by aligning the order tensor principal axes determined from phage media. The structure is aligned to superimpose ring III with that in part a. Note that there is a variation in the apparent orientation of ring II.

approximately 2. In addition, any long-range couplings simply contribute to line broadening in the indirect ^{13}C dimension and have no direct effect on the primary measurements. Spectra are typically recorded with spectral widths of 2000 Hz for the direct proton dimension and 6400 Hz for the indirect carbon dimension, 16 scans per t_1 increment, 512 × 512 complex points, which were linearly predicted to 512 × 800, apodized in both dimensions with a 90° shifted squared sinebell, and zero filled to 1024 × 2048. The couplings were either extracted using a Bayesian time-domain NMR parameter estimation program,[41] Xrambo, or directly measured from the frequency domain.

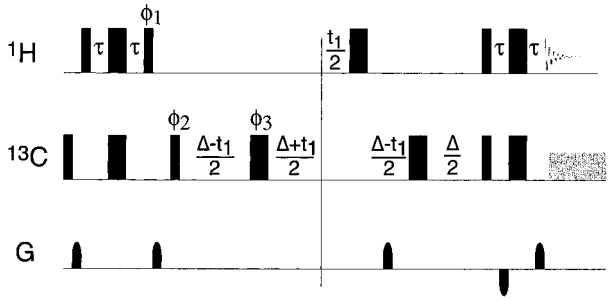

Figure 6. The $^1J_{CH}$(CT-CE-HSQC) experiment. Narrow and wide pulses correspond to 90° and 180° pulses, respectively. The phase cycling is given by $\phi_1\{y, -y\}$, $\phi_2\{x, x, -x, -x\}$, $\phi_3\{x, x, x, x, y, y, y, y\}$, and receiver $\{x, -x, -x, x, -x, x, x, -x\}$. Quadrature is obtained using gradient selection in the usual manner by altering the sign of the gradient in the middle of the indirect evolution period.

The $^1H-^1H$ couplings were measured using constant time COSY (CT-COSY) experiments.[32] As we described before, this experiment allows the active $^1H-^1H$ couplings to be measured in the presence of extensive passive couplings. In the absence of significant differential relaxation, the couplings are obtained from the arctangent of the amplitude ratio of cross-peak (I_{cross}) to auto-peak (I_{auto}) divided by $\pi\Delta$,

$$(J + D) = \arctan(I_{cross}/I_{auto})/\pi\Delta$$

where Δ is the constant time delay. Since the cross-peaks have antiphase character in CT-COSY spectra, a scaling factor (k) is introduced to account for the cancellation effect when integrated intensities are used to represent the cross-peak amplitude. Several spectra were acquired with various constant time delays and the observed intensity ratios were plotted as a function of the constant time delays. The auto-peaks were phased absorptive and directly integrated to represent the autopeak amplitude. For cross-peaks, the positive and negative components of the multiplets are integrated separately and the sum of the absolute intensities of these components is used to represent the cross-peak amplitude. The data were fit allowing simultaneous evaluation of the couplings and the scaling factor. A Mathematica notebook was implemented for this purpose, which also reports the error associated with the curve fitting. Examples of CT-COSY spectra and the curve fittings are provided in Supporting Information. Spectra are typically recorded with spectral widths of 2400 Hz for both direct and indirect proton dimensions, 16 scans per t_1 increment, 1024 × 96 complex points, which were linearly predicted to 1024 × 128, apodized in both dimension with a 90° shifted squared sinebell, and zero filled to 1024 × 256. The constant time delays were 120, 180, 220, 260, 320, 360, 380, and 400 ms for the isotropic sample, 52, 56, 60, 68, 76, and 84 ms for the aligned bicelle sample, and 50, 60, 70, 80, 90, 100, and 110 ms for the phage sample. Water suppression was achieved by presaturation.

Two-bond $^{13}C-^1H$ couplings in the phage aligned sample were measured by an E. COSY-type experiment using a spin-state-selective coherence transfer (S^3CT) pulse element.[33,34] The application of S^3CT generates two subspectra corresponding to the attached ^{13}C spin being in either the α or β state, which makes the coupling measurements easier. Though the spin-state-selective coherence transfer (S^3CT) pulse element is less perfect in selecting spin states in the non-uniform one-bond $^{13}C-^1H$ coupling cases, this effect is expected to be small here: we are measuring the difference of these couplings in isotropic and anisotropic media and the largest one-bond $^{13}C-^1H$ dipolar couplings are less than 10 Hz in phage media. Examples of the spectra are provided in Supporting Information. Spectra were recorded with spectral widths of 2500 Hz for the direct proton dimension and 10000 Hz for the indirect carbon dimension, 24 scans per t_1 increment, 1024 × 360 complex points, were apodized in both dimensions with a 90° shifted

(41) Andrec, M.; Prestegard, J. H. *J. Magn. Reson.* **1998**, *130*, 217−232.

squared sinebell and zero filled to 4096 × 1024. Isotropic mixing of 80 ms was used to achieve the coherence transfer among protons.

Order Matrix Determination from the Residual Dipolar Couplings. The residual dipolar couplings were calculated as the difference of the measured couplings in aligned media (bicelle and phage samples at 36 °C) and isotropic media (bicelle sample at 20 °C). The mannose structure was constructed with use of MacroModel 3.5a.[42] The measured dipolar couplings of each ring and the same molecular coordinates of mannose were separately used as input to a singular value decomposition program,[35] Orderten_SVD, for the determination of the order tensor matrix. The measurement errors of one-bond $^{13}C-^{1}H$ dipolar couplings in the bicelle medium, which aligned to higher order, reported in Table 1 were increased by 50% to account for the uncertainty of the structure in order tensor calculations. Typically 100 000 iterations are performed and the number of accepted solutions was between 1000 and 3000.

Acknowledgment. This work was supported by grants from the NIH (GM33225 and RR05351). We would like to thank Dr. Christian Griesinger for making a copy of a manuscript describing related work on other oligosaccharides available prior to publication.

Supporting Information Available: Three figures showing the measurements of $^{1}H-^{1}H$ dipolar couplings from an CT-COSY experiment and the measurements of two-bond $^{13}C-^{1}H$ dipolar couplings from an E. COSY type experiment (PDF). This material is available free of charge via the Internet at http://pubs.acs.org.

JA002900L

(42) Mohamadi, F.; Richards, N. G. J.; Guida, W. C.; Liskamp, R.; Lipton, M.; Caufield, C.; Chang, G.; Hendrickson, T.; Still, W. C. *J. Comput. Chem.* **1990**, *11*, 440.